Available online www.jsaer.com

***Journal of Scientific and Engineering Research*, 2024, 11(4):85-94**

Research Article

ISSN: 2394-2630
CODEN(USA): JSERBR

Tensile properties stress-strain dynamics simulation of Yima raw coal

MEI Xiangqian[1,2,3*], GONG Jing[1,2,3], CHEN Geng[1,2,3]

[1]State Key Laboratory Cultivation Base for Gas Geology and Gas Control (Henan Polytechnic University), Jiaozuo 454003, China
[2]School of Safety Science and Engineering, Henan Polytechnic University, Jiaozuo 454003, China
[3]Collaborative Innovation Center of Coal Work Safety and Clean High Efficiency Utilization, Jiaozuo 454003, China
Email: mxq6561@163.com

Abstract Molecular dynamics simulation method of LJ potential PCFF force field was used to study the uniaxial tensile and triaxial tensile simulation of *Yima raw coal* at T = 300K, 5×10^{12} s^{-1} strain rate, and triaxial tensile stress-strain response curve of temperature effect at 300-1500K. Then, the stress peaks were fitted by Boltzmann function. The results show that tensile strain will break intermolecular bonds, and temperature increase can promote tensile and bond fracture. At 300K, the stress-strain curves of uniaxial tensile and triaxial tensile have the same trend, but the stress peaks of x-axis and y-axis differ greatly, and the analysis shows that the stress-strain curves roughly conform to the general stress-strain trend, and the peak difference may be the influence of spatial increase. The triaxial tensile stress-strain curve of 300-1500K is more in line with the stress-strain trend of relevant experiments. With the increasing of temperature, the stress curve increases firstly and then begins to decrease after reaching the limit until it approaches 0. The RDF curve also indicates that temperature has an effect on tensile. With the increasing of tensile temperature, the stress peak lower and the strain decrease, indicating that the temperature promotes the simulation process. The fitting effect of stress peak is better (R^2 > 0.9), and the fitting results verify the conclusion. The results can provide reference for tensile simulation of complex polymers and micromolecular study of stress-strain.

Keywords molecular polymers, tensile simulation, temperature, response curve, molecular dynamics

1. Introduction

Coal is the largest energy source in China, and it is more common to analyze the change law of products by experimental means, but the study of coal atomic fracture behavior from the molecular structure [1] [2] has been paid more and more attention. Coal has complex polymer characteristics [3], and the fracture process of polymers is highly dependent on strain [4] [5]. The analysis of stress-strain curve changes by simulation can greatly promote the study of the micromolecular structure of coal.

Molecular dynamics (MD) simulation is one of the experimental methods to characterize material characteristics or verify [6]. The tensile simulation using MD mainly includes metals [7]- [10] and non-metallic polymers [11][12]-[13]; When simulating model tensile, it is divided into uniaxial simulated tensile [10]-[12] and multiaxial spatial simulated tensile [7] [8]. The stress-strain curve generally contains multiple strain stages, and the stress-strain curve [14] and experimental results [15]- [17] are roughly the same under ideal conditions.

At present, the tensile and stress-strain simulation studies are mostly foucused on metal crystals and relatively simple polymers, however, the research on complex high-molecular polymers is relatively lacking. Through tensile simulation of *Yima raw coal* (low-rank lignite), uniaxial tensile and triaxial spatial tensile were

performed at 5×10^{12} s^{-1} strain rate, and the stress-strain curve and stress peak fitting curve of the triaxial spatial tensile process were analyzed by temperature changes. By comparing the difference between the general stress-strain curve and the stress-strain curve of *Yima raw coal* crystal, simulating the stress-strain state and the tensile influence on coal at each stage can provide reference for the tensile simulation of high-molecular polymers.

2. Yima raw coal molecular model

In order to study the stress-strain trend and strain transient phenomenon of *Yima raw coal* during the tensile process, the three-dimensional model of coal is firstly processed. *Yima raw coal* [18] belongs to lignite with low degree of metamorphism, and its molecular formula is $C_{178}H_{146}O_{32}N_2S_2$. Firstly, the three-dimensional model is drawn by Materials Studios software. Then the structure is optimized by the Smart method [19] to reduce the energy of the model to reach the equilibrium state, as shown in Figure . The optimized three-dimensional balance model is shown in Figure.

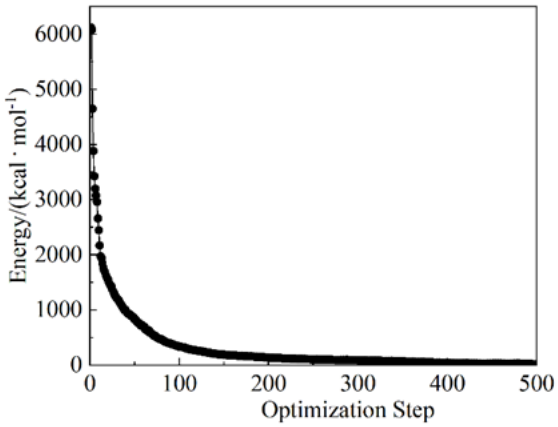

Figure 1: Model energy optimization

The LAMMPS software [20] was used to construct a $30\times30\times10Å^3$ box, and a coal molecular balance model was inserted into the box and the energy minimization was carried out. The LJ potential [21] was selected to describe the interaction between atoms, the general PCFF force field [22] was selected, the periodic boundaries were applied in 3 directions, and the NPT ensemble was loaded before each step of the tensile simulation to perform sufficient relaxation (running 30,000 steps under a timestep of 0.01fs) ,which will ensure that the model reached the specified equilibrium temperature, as Figure. So that the initial structure is rationalized, and the optimized model is visualized with Ovito software [23], as shown in Fig.

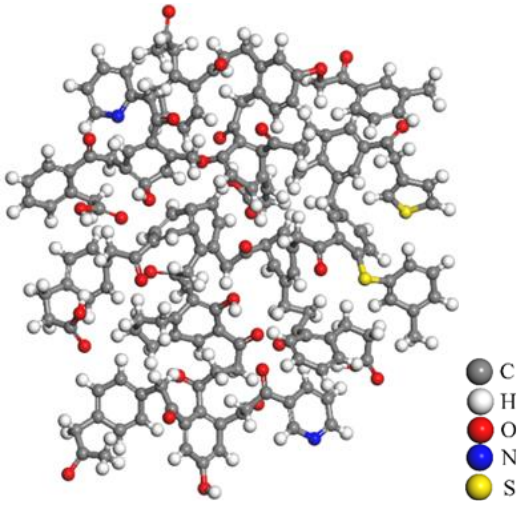

Figure 2: Three-dimensional equilibrium structure of Yima raw coal

After relaxation, the model was simulated of which x-axis, y-axis, and z-axis uniaxial tensile and xyz triaxial spatial tensile at 5×10^{12} s^{-1} strain rate and 300K temperature. Then the controlling the triaxial tensile temperature was carried out to 600K, 900K, 1200K and 1500K. The results are visualized and analyzed by Ovito software. By originating the stress-strain data of the tensile process, the stress-strain curve and the stress peak fitting curve are will analyzed.

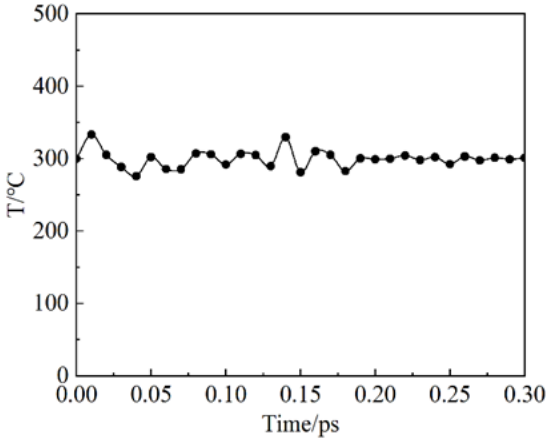

Figure 3:The model simulates temperature changes over time

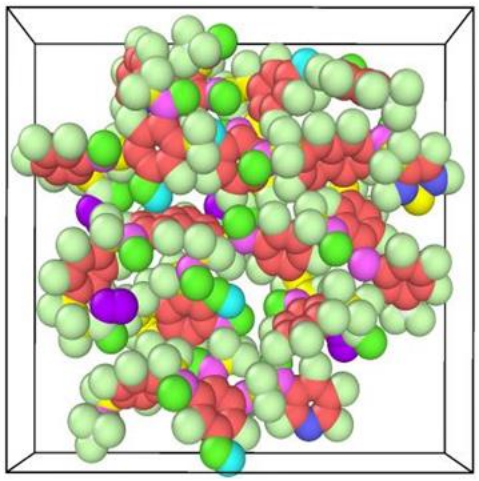

Figure 4: Relaxation balance diagram of Yima raw coal

3. Coal molecular tretching simulation

3.1 Uniaxial tensile

For the relaxed model at 300K and 5×10^{12} s^{-1} strain rate, the x-axis, y-axis, and z-axis uniaxial tensile was performed with the timestep of 0.01fs and running 100,000 steps. Dealing with the results has obtained the stress-strain curves (see Figure) and the tensile instantaneous diagram (see Figure).

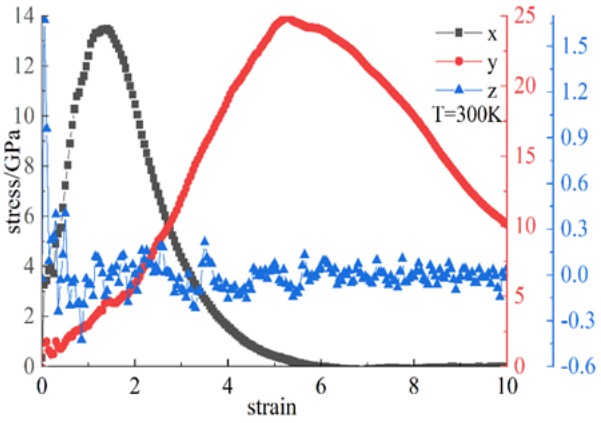

Figure 5: Uniaxial tensile stress-strain curve

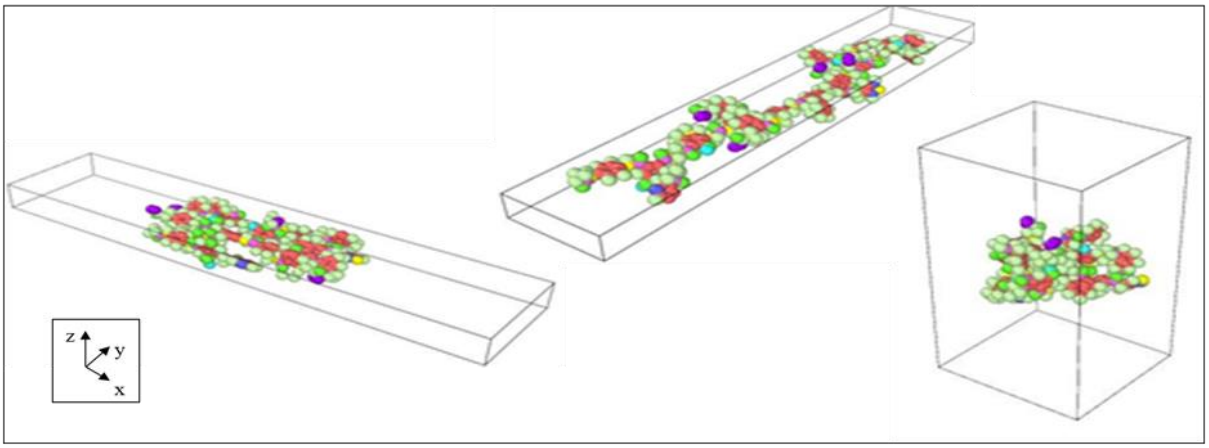

Figure 6: Instantaneous strain trend of uniaxial tensile

From Figure, it can be seen that the x-axis tensile reaches the stress peak faster than the y-axis when the temperature and strain rate are constant, but the difference in peak size is not large. The z-axis stress-strain curve has a large fluctuation range, which is different from the idealized stress-strain curve. The possible reason is that the model is amorphous, which makes the coal molecules and the cell body misaligned at the moment of tensile, resulting in different levels of stress great change in the three axes at the beginning of strain. And z-axis, because the distance is the smallest, has the largest degree of giant change, resulting in large stress fluctuations when subsequent strains are imposed.

As can be seen from Figure, the z-axis tensile trend is relatively small and inversely the y-axis tensile trend is the largest under the same strain. It is due to the distance between x-axes and y-axes being 30Å, which is larger than the z-axis, resulting in a smaller increase in z-axis tensile. The y-axis tensile trend is larger than the x-axis, which is consistent with the fact that the y-axis transient stress is smaller than the x-axis when the strain is initially imposed. The instantaneous stress at the zero point is too large, resulting in a large trend of the crtstal and box separation. When the overall model increase is constant, the crtstal increase is relatively small.

3.2 Triaxial tensile

To compare the similarities and differences of stress-strain trends between uniaxial tensile and triaxial tensile of the model, triaxial tensile simulations were performed at 5×10^{12} s^{-1} strain rate and 300K temperature with the timestep of 0.01fs and running 100,000 steps. Then the stress-strain curves (see Figure) and the different strain instantaneous (see Figure) were obtained.

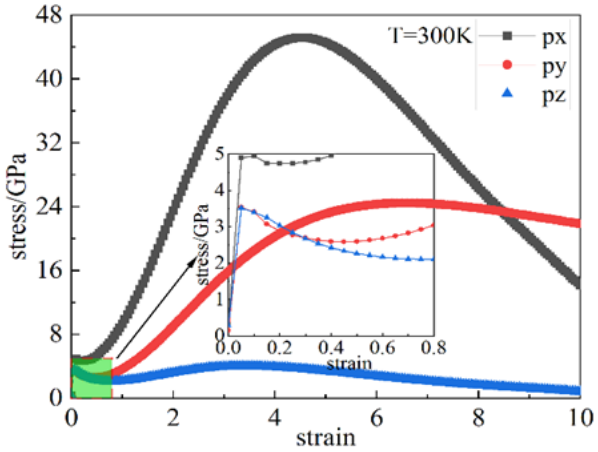

Figure 7:Triaxial tensile stress-strain curve at 300K

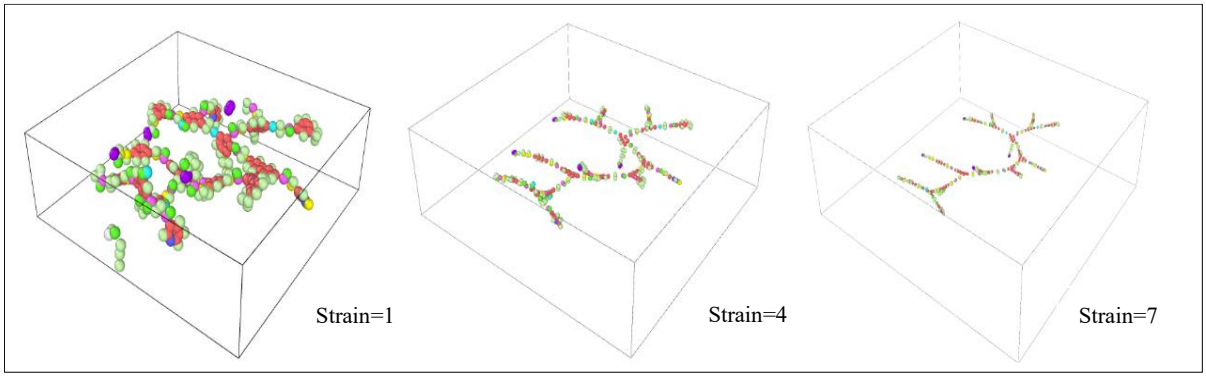

Figure 8: Instantaneous tensile of different strains during triaxial tensile

In Figure, selecting three strain instantaneous states from the 10 strains, it is found that the coal molecules have been displacing and cracking. As the strain increases, the model space size becomes more and more larger and the coal molecules are stretched more and more seriously. It results in the intermolecular forces being broken by the tensile stress, thus breaking the intermolecular bonds of coal. So the stress-strain tensile promotes intermolecular bond fracture [4] [5].

As can be seen from Figure, the stress peak is reached in all three axes within 10 strains. The x-axis stress peak is the largest, the z-axis is the smallest, and the z-axis peak is the smallest in agreement with the uniaxial tensile result. X-axis stress peak is nearly twice as large as the y-axis, and the strain reaching the peak in the x-axis is expanded nearly two times compared to the uniaxial tensile, which is close to the strain value of the y-axis peak. The possible reason is that in uniaxial tensile, the direction of strain is unique and the model increase is in one plane, while in triaxial tensile, the strain is stretched in three planes simultaneously and the model increase is a spatial increment. That leads to the difference in the tensile results. Meanwhile, the instantaneous diagram of the initial strain increment reveals that at the instant of the beginning of triaxial tensile, the stress changes dramatically, resulting in a non-zero stress, which is consistent with the conclusion of the CT scan triaxial compression experiment [16]; subsequently, as the strain increases, the model gradual is stretched. And the stress-strain response trend gradually conforms to the experimental test results [15] [16].

4 Tensile analysis of temperature change

4.1 Effect of temperature on tensile

Temperature have some extent effect on the model tensile [7] [13], [24]. In order to analyze the effect of temperature on the stress-strain during the process of coal tensile, triaxial spatial tensile simulations at T = 600, 900, 1200 and 1500K were performed for the above model on the basis of T = 300K. In order to make the tensile temperature constant, relaxation treatment was performed before tensile to bring the models to their

respective equilibrium temperatures. The stress-strain curves at different temperatures were obtained for the same timestep and running steps (see Figure).

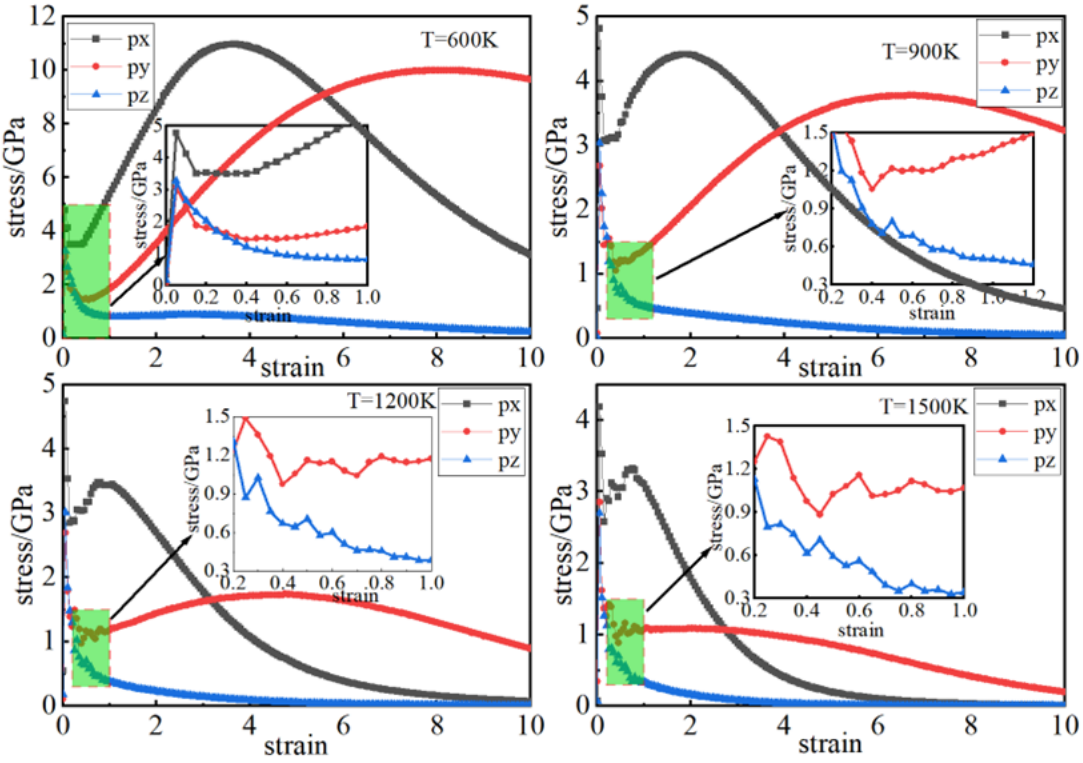

Figure 9: Triaxial tensile stress-strain curves at different temperatures

It can be seen that the strain of x-axis, y-axis, and z-axis when they reach the stress peak decreases with the tensile temperature increases. And the stress peak also decreases gradually. That indicats the temperature promotes the fracture of coal molecules [25] [26]. It can be found that at the instant of the initial strain increase, all three axes of stress appear huge fluctuations, which can be considered as the occurring physical destruction of strain. With the increase of strain, the stress curve gradually increases firstly and then decreases until it tends to 0. During this process, the coal sample begins to produce irreversible plastic deformation, and when the stress reaches the strength limit, the coal sample undergoes destabilization damage [16]. Compared to the x-axis stress peak with the increase of temperature leading to strain decrease, the y-axis peak strain at 300-600K temperature is increasing, on the contrary, the peak strain at 600-1500K temperature is decreasing, probably because the y-axis is subjected to the force degree higher than the x-axis. While the z-axis with the increase of temperature, the stress peak appears less obvious and more fluctuates, the same trend with uniaxial tensile. In addition to the smaller distance of the z-axis is one of the influencing factors, the deeper reasons need to be further explored.

Analyzing the temperature effect on stress-strain at 300-1500K, it is found that the stress peak in x-axis reaches 45.17GPa at 300K and 10.97GPa at 600K, shrinking by about 3/4, and the peaks in 900-1500K are all lower than 5Gpa. The y-axis go from 24.46GPa at 300K to 10.01GPa at 600K, shrinking by nearly 3/5, and then the stress peaks with temperature increases are also below 5GPa. Although the stress peaks in the x-axis and y-axis are different, the overall change trend is the same, and this trend is also found in the z-axis, which is consistent with the general trend of the relevant experimental findings [15]-[17] and simulation conclusions [11][12]-[13].

4.2 Radial distribution function analysis

The Radius distribution function (RDF) is an effective method to study the distribution probability of particles in space with the variation of distance, commonly used to study the ordering within matter [7] and to identify different atomic structures [27]. To fit the truncation radius less than half of the minimum side length of the box, the RDF of r = 5Å is taken. Then the image of the RDF of the overall model at 300-1500K temperature is plotted (see Figure).

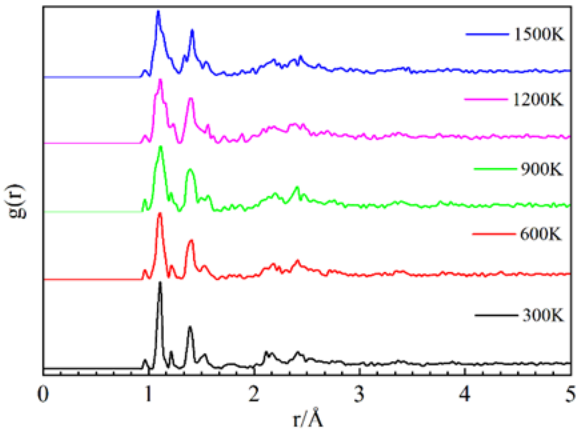

Figure 10: Variation of radius distribution function at 300-1500K temperature

It shows that the images of the RDF at 300-1500K temperature have roughly the same trend, and the first peak appears at r = 0.95Å, which is a short-range peak, because the model is amorphous and does not have a long-range peak. At the same time, the RDF also occurs change of different degrees with the increase of temperature, taking the second peak (the highest peak) as an example: at 300K, the highest peak appears at r = 1.10Å, and the peak reaches 25Å, but the peak is relatively narrow. When the temperature increases, the radius of the highest peak appearance are the same, but the peak height gradually decreases and the peak gradually becomes wider. Meanwhile, the peak appears with high frequency and fluctuation phenomenon before r = 2.85Å. However, the peak wave tends to smooth gradually after r = 2.85Å. Therefore, the RDF also indicates that the temperature has an effect on tensile.

4.3 Stress peak fitting analysis

In order to better observe the effect of temperature on the stress peak, the triaxial tensile stress peak was fitted to the temperature effect at 300-1500K.

The choice of the fitting function is crucial when fitting the stress peaks, and the peak data were pre-analyzed and found not to follow a linear trend. The Boltzmann function [28] of equation (1) is a nonlinear fitting function, and the fitted curve has a high correlation coefficient and can be better fitted in the case of large numerical dispersion. Therefore, the Boltzmann function was used to fit the stress peak and the results were optimized (see Figur and Figure).

$$y = A_2 + \frac{A_1 - A_2}{1 + \exp((x - x_0)/dx)} \quad (1)$$

Figur shows R^2 = 0.998554 > 0.9, indicating a good fit effect that the stress peak decreases as the strain reduces, and Figure also has the same effect. As the temperature increases, the stress peak decreases and the strain also reduces, but the A_2 value of the x-axis fitted curve is much larger than that of the y-axis and z-axis. Because the peak value of the x-axis is 45.17GPa at 300K, which is much higher than that of the y-axis and z-axis, resulting in its y-axis intercept being the largest.

At the same time, since the R^2 of the three-axis fit is greater than 0.9, it can be seen that the fit effect is ideal. While both the y-axis and z-axis have a deviation point (the red points in Figure) that are ignored during the fitting, resulting in the fitted R^2 (R_y^2 = 0.95452，R_z^2 = 0.92158) being smaller than the x-axis (R_x^2 = 0.99854). It also shows that the peak occurs with strain magnitude: y>x>z; and stress magnitude: x>y>z.

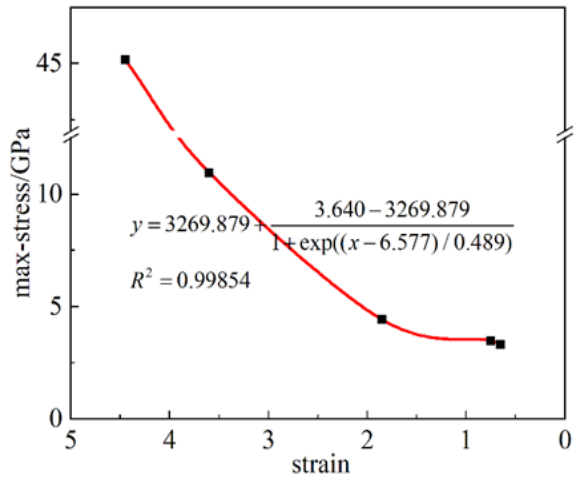

Figure 11: X-axis stress peak fitting at 300-1500K

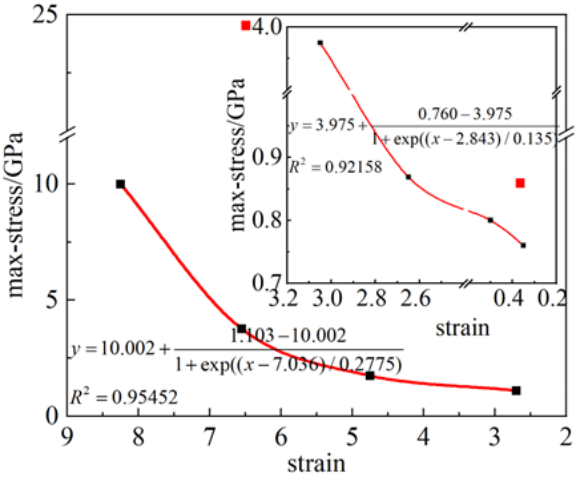

Figure 12: Peak fitting of stress in y-axis and z-axis at 300-1500K

5. Conclusion

By simulating uniaxial and triaxial tensile of complex molecule polymer *Yima raw coal* and adding temperature variables, analyzing the stress-strain response curve of the tensile process and the structural tensile instantaneous strain, and fitting Boltzmann function to the stress peak at 300-1500K temperature, the results show that:

1) The tensile process will occur intermolecular bond rupture phenomenon, when the strain increases the tensile will be more obvious, and the temperature increase promotes tensile and bond rupture. While the strain increases transiently from 0 will lead to the relative displacement of coal molecules and boxes, prompting sudden changes of stress.
2) At 300K temperature and 5×1012 s-1 strain rate, the stress-strain curves of uniaxial tensile and triaxial tensile have the same trend overall, but the stress peak of x-axis tensile has large difference. While the x-axis and y-axis stress peaks are similar in uniaxial tensile, the peak difference is nearly 2 times in triaxial tensile, which may be the effect of spatial tensile increase.
3) The triaxial tensile trend of stress-strain curve at 300-1500K temperature effect is roughly in line with the general stress-strain trend, and the RDF indicates that temperature has an effect on tensile. With the increase of temperature, the stress peak decreases and the strain reduces, and the stress peak fitting results verify the conclusion.

Data Availability

The data used to support the conclusion of this study are available from the corresponding author upon request.

Conflicts of Interest

The authors declare that they have no conflicts of interest.

References

[1] Zhang M, Li X, Nie F, et al. Investigation of overall pyrolysis stages for Liulin bituminous coal by Large-Scale ReaxFF molecular dynamics. Energy & Fuels 2017; 31(4): 3675-3683.

[2] Xu F. Construction of molecular model of Lignite in Huolin River and molecular dynamics simulation of pyrolysis reaction. Harbin Institute of Technology 2020.

[3] Cheng N N, Shi M Y, Hou Q L, et al. Application of Raman spectroscopy in the characterization of coal macromolecular structure. Journal of China Coal Society. Epub ahead of print 8 April 2022. DOI: 10.13225/j.cnki.jccs.2021.1730.

[4] Hyon J, Lawai O, Fried O, et al. Extreme energy absorption in glassy polymer thin films by supersonic micro-projectile impact. Materials Today 2018; 21(8): 817-824.

[5] Yeh, I.-C, Andzelm, et al. Mechanical and structural characterization of semicrystalline polyethylene under tensile deformation by molecular dynamics simulations. Macromolecules 2015; 48: 4228-4239.

[6] Park C, Jung J and Yun G J. Thermomechanical properties of mineralized nitrogendoped carbon nanotube/polymer nanocomposites by molecular dynamics simulations. Composites Part B: Engineering 2019; 161: 639-650.

[7] Wang Y T, Zeng X G and Yang X. Molecular dynamics of the effect of temperature on pore nucleation and growth in single crystal iron under high strain rate. Acta Physica Sinica 2019; 68(24): 235-251.

[8] Sunil Kumar. Evolution of nano-porous structure of aluminium-magnesium alloy during multi-axial tensile deformation: Estimation of stress-strain response and dimension-less aspect ratio. Materials Chemistry and Physics 2018; 220: 50-57.

[9] Vu T N, Pham V T and Fang T H. Influences of grain size, temperature, and strain rate on mechanical properties of Al0. 3CoCrFeNi high–entropy alloys. Materials Science and Engineering: A 2022; 858: 144158.

[10] Mahdi J, Mohammad S G. Nanovoid induced martensitic growth under uniaxial stress: Effect of misfit strain, temperature and nanovoid size on PT threshold stress and nanostructure in NiAl. Computational Materials Science 2020; 184: 109928.

[11] Chen S H, Lv Q, Guo J C, et al. Molecular dynamics simulation of graphene/polyethylene composites and their tensile properties. Acta Polymerica Sinica 2017; (04): 716-726.

[12] Li X L, Guo J G. Theoretical study on uniaxial compressive mechanical properties of three-dimensional graphene. International Journal of Mechanical Sciences 2023; 249: 108250.

[13] Bowman A L, Mun S, Huddleston B D, et al. A nanoscale study of size scale, strain rate, temperature, and stress state effects on damage and fracture of polyethylene. Mechanics of Materials 2021; 161: 104008.

[14] Liu H, Wu F Y, Zhong G J, et al. Predicting the complex stress-strain curves of polymeric solids by classification-embedded dual neural network. Materials & Design 2023; 227: 111773.

[15] Zhang B Y, Yu Y, Gao X, et al. Experimental study on stress-strain characteristics of coal containing gas hydrate under unloading confining pressure. Journal of China Coal Society 2021; 46(S1): 281-290.

[16] Wang D K, Wu Y, Wei J P, et al. Dynamic evolution characteristics of gas-bearing coal fractures based on grayscale symbiotic matrix and industrial CT scan. Chinese Journal of Engineering 2023; 45(01): 31-43.

[17] Liu H Q, Bai G L, Wang J W, et al. Experimental study on uniaxial compressive stress-strain curve of gangue concrete. Journal of Building Structures. Epub ahead of print 16 September 2022. DOI: 10.14006/j.jzjgxb.2022.0279.

[18] Wang S Y. Molecular dynamics simulation and quantum chemistry study of lignite structure. Taiyuan University of Technology 2004.

[19] Lu H, Zhou Z, Hao T, et al. Temperature dependence of structural properties and chain configurational study: a molecular dynamics simulation of polyethylene chains. Macromolecular Theory and Simulations 2015; 24(4): 335-343.
[20] Plimpton S. Fast parallel algorithms for short-range molecular dynamics. Journal of computational physics 1995; 117(1): 1-19.
[21] Etienne Cuierrier, Sadollah Ebrahimi, Olivier Couture, et al. Simulation of main chain liquid crystalline polymers using a Gay-Berne/Lennard-Jones hybrid model. Computational Materials Science 2021; 186: 110041.
[22] Sun H, Mumby S J, Maple J R, et al. An ab initio CFF93 all-atom force field for polycarbonates. Journal of the American Chemical society 1994; 116(7): 2978-2987.
[23] Stukowski A. Visualization and analysis of atomistic simulation data with OVITO–the Open Visualization Tool. Modelling and simulation in materials science and engineering 2009; 18(1): 015012.
[24] Lu Y J, Chen S W and Zhang Y. Tensile mechanical properties and constitutive relationships of ionic interlayers at medium and high strain rates and different temperatures. Engineering Mechanics 2021; 38(02): 101-109.
[25] Li Y, Wan K D, Zhang K, et al. Model prediction and experimental study on the influence of cracking temperature on pulverized coal cracking characteristics. Journal of China Coal Society 2017; 42(07): 1870-1876.
[26] Silvera Scaccia. Analysis and distribution of volatile gases from catalytic pyrolysis of Sulcis low-rank coal. Journal of Analytical and Applied Pyrolysis 2023; 169, 105820.
[27] Tang J, Ahmadi A, Alizadeh A, et al. Investigation of the mechanical properties of different amorphous composites using the molecular dynamics simulation. Journal of Materials Research and Technology 2023; 24: 1390-1400.
[28] Lu Q, Zhang Z H, Zhang W P, et al. Point Extension Function Model of Grating Imaging System Based on Boltzmann Function Edge-Edge Fitting . Acta Optica Sinica 2020; 40(14): 32-39.